Carcinogenesis vol.32 no.8 pp.1167–1175, 2011
doi:10.1093/carcin/bgr101
Advance Access publication June 3, 2011

Hypoxia-increased RAGE and P2X7R expression regulates tumor cell invasion through phosphorylation of Erk1/2 and Akt and nuclear translocation of NF-κB

Marco Tafani[1,*], Luana Schito[1,2], Laura Pellegrini[1], Lidia Villanova[1], Gabriella Marfe[3], Tahira Anwar[4], Roberta Rosa[5], Manuela Indelicato[6], Massimo Fini[6], Bruna Pucci[6] and Matteo A.Russo[1,6]

[1]Department of Experimental Medicine, Sapienza University, 1, 00161 Rome, Italy, [2]Department of Medicine, Institute of Genetic Medicine, Johns Hopkins University School of Medicine, The Johns Hopkins University, Baltimore, MD 21205, USA, [3]Department of Experimental Medicine and Biochemical Sciences, University of Rome "Tor Vergata", 00133 Rome, Italy, [4]Department of Biosciences Division of Biochemistry, University of Helsinki, Helsinki 00100 Finland, [5]Department of Molecular and Clinical Endocrinology and Oncology, University of Naples ''Federico II'', 80138 Naples, Italy and [6]Department of Cellular and Molecular Pathology, IRCCS San Raffaele Pisana, 00163 Rome, Italy

[*]To whom correspondence should be addressed. Tel +39 06 49970665; Fax: +39 06 49970806;
Email: marcotafani@yahoo.com

The role of hypoxia in regulating tumor progression is still controversial. Here, we demonstrate that, similarly to what previously observed by us in human prostate and breast tumor samples, hypoxia increases expression of the receptor for advanced glycation end products (RAGE) and the purinergic receptor P2X7 (P2X7R). The role of hypoxia was shown by the fact that hypoxia-inducible factor (HIF)-1α silencing downregulated RAGE and P2X7R protein levels as well as nuclear factor-kappaB (NF-κB) expression. In contrast, NF-κB silencing reduced P2X7R expression without affecting RAGE protein levels or nuclear accumulation of HIF-1α. Treatment of hypoxic tumor cells with HMGB1 and BzATP ligands, respectively, of RAGE and P2X7R, activated a signaling pathway that, through Akt and Erk phosphorylation, determines nuclear accumulation of NF-κB and increases cell invasion. Inhibition of Akt by SH5 and Erk by INH1 prevented both nuclear translocation of NF-κB and cell invasion. Moreover, silencing RAGE and P2X7R abolished nuclear accumulation of NF-κB as well as cell invasion without affecting HIF-1α stabilization. Once in the nucleus, NF-κB would contribute to cell survival and invasion under hypoxia, by maintaining RAGE and P2X7R expression levels and matrix metalloproteinases 2 and 9 synthesis. These results show that, hypoxia can upregulate expression levels of membrane receptors that, by binding extracellular molecules eventually released by necrotic cells, contribute to the increased invasiveness of transformed tumor cells. Moreover, these observations strengthen our working hypothesis that upregulation of damage-associated molecular patterns receptors by HIF-1α represents the crucial event bridging hypoxia and inflammation in obtaining the malignant phenotype.

Introduction

Hypoxia occurs while transformed cells in a tumor are growing in the absence of neoangiogenesis. At a cellular level, the drop in oxygen concentration has two important consequences: activation of hypoxia-inducible factor-1 (HIF-1) and necrosis of cells that are distant from blood supply. HIF-1 is a heterodimeric protein composed by two subunits α and β. Under normoxia, HIF-1α is degraded by the ubiquitin–proteasome system, but when the intracellular oxygen concentration drops, HIF-1α is stabilized (1). Following stabilization, HIF-1α translocates to the nucleus where it binds to HIF-1β. The HIF-1α and β dimer activates the expression of vascular endothelial growth factors and their receptors (2), change in energy metabolism (3) and upregulation of RAGE (4). At the same time, necrosis causes a release of intracellular alarmins also called damage-associated molecular patterns (DAMPs) that, by binding to different receptors activates nuclear factor-kappaB (NF-κB) triggering the inflammatory response (5). RAGE and purinergic receptor P2X7 (P2X7R) represent two plasma membrane receptors able to bind DAMPs released by necrotic cells.

The receptor for advanced glycation end products (RAGE) is a transmembrane receptor classified as an immunoglobulin super family member. RAGE is expressed by numerous cell types including monocytes, macrophages, T-lymphocytes, neurons, endothelial cells, osteoclasts, osteoblasts and a variety of cancer cells (6–11). RAGE expression is stimulated by different stressing stimuli with hypoxia being one of them (4). In fact, RAGE expression levels increased in neuron under hypoxia through the binding of the HIF-1 (4). Once expressed, RAGE binds to several ligands including advanced glycation end products, high mobility group box 1 protein (HMGB1), S100 proteins and amyloid β-fibrils. RAGE signal transduction pathways typically activate NF-κB-mediated responses involved in inflammatory gene expression and this receptor plays a significant role in the alarmin response of the innate immune system and contributes to diabetic complications and neurodegenerative disorders (12,13). Furthermore, elevated expression levels of RAGE have been detected in a large number of tumors (14,15). Therefore, RAGE is considered as a receptor capable of bridging inflammation and cancer (16,17). In fact, recent studies, starting from the fact that chronic inflammation is a major causative factor in many human malignancies, have shown a correlation between RAGE expression and tumor progression (18–20). For example, blockade of RAGE signaling by multiple strategies prevented tumor growth and metastasis formation in severe combined immune deficient mice (21).

The P2X7R is an adenosine triphosphate (ATP)-sensitive, ligand-gated ion channel that functions as a nonselective cation channel and, upon prolonged agonist exposure, leads to the formation of progressively enlarged cytolytic pores (∼900 Da) on the cell surface (22,23). Seven different P2X receptor subtypes have been molecularly defined arising from distinct genes (24). P2X receptors bear common topology, containing intracellular N and C termini, two transmembrane domains and a large extracellular loop. Among P2X receptors, P2X7R appears to be the most divergent member (25) since it requires high concentrations of ATP to be activated (typically present in a microevironment where cells are dying by necrosis). Furthermore, P2X7 has been shown to be specifically involved in mediating ATP-induced apoptosis of several cell lines (26–29). Such cytotoxic effect of P2X7R has been widely studied and considered to be a promising therapeutic tool to activate cell death in tumorigenic cells by exposing them to increasing doses of ATP (30). However, recently, a different approach has been taken where this same P2X7R has been shown to possess survival/growth-promoting effects under physiological conditions as extensively reviewed by Di Virgilio *et al.* (31). In fact, transfection of P2X7R in several cell lines increases their growth, whereas growth arrest of microglia is accompanied by a down-modulation of P2X7R levels. Moreover, P2X7R expression has been shown to be increased in several malignant tumors such as prostate, breast carcinoma, neuroblastoma, leukemia and thyroid papillary carcinoma (31–33). However, the expression levels of P2X7R in the presence of hypoxia as well as the benefits of the increased P2X7R expression for the growth and progression of tumor cells have never been investigated.

Abbreviations: ATP, adenosine triphosphate; DAMP, damage-associated molecular pattern; HIF, hypoxia-inducible factor; HMGB1, high mobility group box 1 protein; MMP, matrix metalloprotein; NF-κB, nuclear factor-kappaB; P2X7R, purinergic receptor P2X7; RAGE, receptor for advanced glycation end products; shRNA, short hairpin RNA.

We have recently shown that a proinflammatory-reparative response is activated in tumor samples of prostate and breast carcinomas in the absence of a leukocyte infiltrate (18,19). In fact, isolation of tumor and host cells from these tumor samples by laser capture microdissection led us to observe an increased and coordinated expression of several proinflammatory proteins only in tumor cells (18,19). Recently, we have observed an upregulation of proinflammatory proteins in human glioblastoma multiforme biopsies as well as in tumor stem cells obtained from these same samples (34). We concluded that hypoxia induces in tumor cells, a coordinated proinflammatory gene response (similar to that of DAMPs or alarmin-activated leukocytes), leading to crucial biological properties needed for invasion, migration and probably specific homing.

Aim of this study was to demonstrate that expression of the RAGE and the P2X7R is upregulated by hypoxia. Moreover, we wanted to show that, once upregulated, these two receptors play an important role in tumor cell invasion and migration.

Here, we show that in MDA-MB-231, MCF-7 and HeLa cells, RAGE and P2X7R expression levels are increased by hypoxia through HIF-1α. In particular, tumor cells with increased RAGE and P2X7R respond to extracellular ligands (HMGB1 and BzATP) by activating intracellular pathways that, through Akt and/or Erk1/2 activation, cause nuclear translocation of NF-κB. Once in the nucleus, NF-κB helps to maintain expression of RAGE and P2X7R. Furthermore, our study shows that hypoxia-driven increase of RAGE and P2X7R enhances invasion and migration of tumor cells.

Materials and methods

Cell cultures

The MDA-MB-231 and MCF-7 breast carcinoma cell lines as well as the cervical cancer HeLa cell line (American Type Culture Collection-LGC standards, Milan, Italy) were maintained in 75 cm^2 polystyrene flasks (Corning Costar Corporation, Oneonta, NY) with RPMI 1640 medium (Mediatech, Herndon, VA), containing 100 U/ml penicillin, 0.1 mg/ml streptomycin and 10% heat-inactivated fetal bovine serum. The cells were incubated under an atmosphere of 95% air and 5% CO_2. The cell lines were maintained in culture for <6 months after resuscitation. The cell lines were tested by ATTC–LGC cell bank through genomic, proteomic and immunology procedures as indicated by the company (authentication technology; ATCC–LCG).

Treatment protocols and antibodies

In all experiments, HMGB1 (Sigma, St Louis, MO) was dissolved in water and added to a final concentration of 100 ng/ml. BzATP (Sigma–Aldrich, St Louis, MO) was dissolved in, dimethyl sulfoxide (Me_2SO) and added to a final concentration of 50 nM. Cell permeable ERK Activation Inhibitor Peptide I (INH1) and cell permeable Akt inhibitor II (SH5) (Merck Chemicals, Nottingham, UK) were dissolved in dimethyl sulfoxide and added to a final concentration of 2.5 and 10 μM, respectively. Control experiments showed that Me_2SO had no effect on any of the parameters measured. The following primary antibodies were used: mouse anti-HIF-1α antibody (BD Bioscience, San Jose, CA), mouse anti-NF-κB p65 (Santa Cruz Biotechnology Inc., Santa Cruz, CA), mouse anti-IKBKB (Sigma–Aldrich), rabbit anti-RAGE (Aviva System Biology, San Diego, CA), rabbit anti-P2X7R (Santa Cruz, CA), rabbit anti-Akt and anti-phospho-Akt (Ser473), (Thr308) (Santa Cruz, CA), rabbit anti-ERK1/2 and anti-phospho-ERK1/2 (Tyr202/Thr204) (Invitrogen, Milan, Italy), mouse anti-Lamin A/C antibody (BD Bioscience) and mouse anti-β actin (Santa Cruz, CA). The following secondary antibodies were used: mouse anti-rabbit horseradish peroxidase, goat anti-mouse horseradish peroxidase (Amersham Biosciences, Piscataway, NJ).

Hypoxia

Hypoxic conditions were achieved by incubating cells in a hypoxia chamber (Billups-Rothenberg, Del Mar, CA) where a 1% oxygen mix was flushed in for 4 min according to the manufacturer's instructions.

Isolation of cytosol and nuclear fractions

Cells (2×10^6) were plated in 100 mm dishes. The nuclear and cytosolic fractions were isolated using the nuclear extraction kit from Active Motif (Carlsbad, CA), following manufacturer's instructions. Briefly, following treatment, cells were scraped off the plate in a phosphate-buffered saline/phosphatase inhibitor buffer using a rubber policeman. Cells were centrifuged 5 min at 500 r.p.m. at 4°C and the supernatant discarded. The cell pellet was lysed in hypotonic buffer for 15 min in ice followed by centrifugation (30 s at 14 000 r.p.m. at 4°C). The supernatant (cytosolic fraction) was transferred to a new tube, whereas the pellet (nuclear fraction) was lysed in a lysis buffer in the presence of protease inhibitors. The cytosolic fraction was concentrated through a Microcon YM-10 Centrifugal Filter Device (Millipore, Bedford, MA). Protein concentration of the fractions was determined by the Bradford assay (Bio-Rad, Hercules, CA).

Western blot assay

Cells (1×10^6) for whole cell lysate were collected in a phosphate-buffered saline/phosphatase inhibitor buffer using a rubber policeman, pelleted, centrifuged at 700*g* (5 min at 4°C) and lysed in 50 μl of cell lysis buffer (20 mM Tris, pH 7.4, 100 mM NaCl, 1% Triton, 1 mM phenylmethylsulfonyl fluoride, 10 μg/ml leupeptin, 10 μg/ml aprotinin). After 30 min on ice, the lysates were clarified by centrifugation (10 min at 14 000 r.p.m. at 4°C) and the supernatant was collected. Protein concentration was determined by the Bradford assay (Bio-Rad). Equivalent amounts of protein were electrophoresed on sodium dodecyl sulfate–polyacrylamide gels. Kaleidoscope Prestained Standards (Bio-Rad) were used to determine molecular weight. The gels were then electroblotted onto polyvinylidene difluoride membranes. After blocking with 5% milk, membranes were incubated with the primary antibody overnight. Finally, the relevant protein was visualized by staining with the appropriate secondary horseradish peroxidase-labeled antibody for 1 h followed by enhanced chemiluminescence. Digital images of the resulting bands were quantified by the Quantity One software package (Bio-Rad Laboratories, Munchen, Germany) and expressed as arbitrary densitometric units.

HIF-1α, IKBKB, P2X7R and RAGE short hairpin RNA lentivirus transduction

Mission™ TRC short hairpin RNA (shRNA) lentiviral transduction particles expressing shRNA-targeting HIF-1α, IKBKB, P2X7R or RAGE and lentiviral-negative control particles were purchased from Sigma–Aldrich. Stably transduced clones were generated according to the manufacturer's instructions. Briefly, cells were seeded on a 24-well plate. The following day cells were infected. After 24 h, medium was changed with fresh RPMI. Selection of stable clones was started 24 h later with the addition of 3 μg/ml of puromycin. The expression of HIF-1α, IKBKB, P2X7R and RAGE was confirmed by western blotting.

Cell invasion assay

Cell invasion was measured using the 24-well cell invasion assay kit from Chemicon following manufacturer's instructions. The kit is designed to discriminate between invading and non-invading cells with only the former being able to digest an extracellular matrix, migrate through the pores and cling to the membrane. Briefly, an equivalent number of cells either treated or not-treated was resuspended in serum-free medium supplemented with 1% bovine serum albumin and seeded in an insert. The insert was then placed inside a 24-well plate. Each well was filled with 500 μl of serum-free medium supplemented with 1% bovine serum albumin and a chemoattractant. The plate was incubated in normoxia or hypoxia for the indicated time to allow for the invasion and migration of the cells. Subsequently, the insert was placed in a dye solution to stain the cells and then scraped with cotton swabs to remove the non-invading cells at the top of the membrane. Pictures of the cells at the bottom of the membrane were taken with a digital camera mounted on an EclipseNet 2000 microscope (Nikon Instruments, Firenze, Italy). Alternatively, in a separate set of experiments, stained cells were dissolved in 200 μl of 10% acetic acid solution (Sigma) for 10 min. Afterward, 100 μl of dye/solute mixture was transferred into a 96-well plate for colorimetric reading of optical density at 560 nm.

Zymography

Cells (10^6) were plated in RPMI medium without serum and 1% bovine serum albumin to remove the metalloproteinase activity present in the fetal bovine serum. The day after, cells were either left untreated or treated as indicated in the figure legend. At the end of the treatment, the cellular supernatant was collected, centrifuged at 10 000 r.p.m. for 5 min at 4°C and stored at −80°C. The day of the experiment, the supernatant was concentrated with Microcon YM-10 filters (Millipore, Milan, Italy) and the protein content determined by the Bradford assay (Bio-Rad). An equivalent amount of protein was loaded on a 10% polyacrylamide gel containing 2 mg/ml of gelatin and separated by electrophoreses. Afterward, the gel was washed 30 min in 2% Triton and incubated in the proteolytic buffer (50 mM Tris/HCl, 0.15 M NaCl, ZnCl 1 mM, pH 7.7) for 20 h at 37°C to allow the matrix metalloproteinase (MMP) digestion of the gelatine substrate. The day after, the gel was washed with a 20% trichloroacetic acid solution, stained in a buffer containing 70% methanol, 20% acetic acid, 1 g Coomassie Blue and destained in a solution with 70% methanol, 20% acetic acid. After destaining, the areas where the MMP-2 and -9 have digested the gelatine substrate appeared as white lanes on a blue background.

Statistical analysis

The results are expressed as means ± standard deviations and 95% confidence intervals. Before using parametric tests, the assumption of normality was verified using the Shapiro–Wilk *W*-test. Student's paired *t*-test was used to determine any significant differences before and after treatment. Significance was set at 0.05 ($P \leq 0.05$). SPSS statistical software package (Version 13.0.1 for Windows; SPSS, Chicago, IL) was used for all statistical calculations.

Results

Hypoxia increases RAGE and P2X7R expression through HIF-1α

The expression of the two alarmin receptors RAGE and P2X7R in MDA-MB-231, MCF-7 and HeLa cells was increased by hypoxia (Figure 1A). In particular, in MDA-MB-231 and HeLa cells, RAGE increase was visible after 4 h and maintained up to 24 h of hypoxia, whereas in MCF-7 cells, RAGE expression was increased after 8 h of hypoxia. The increase in P2X7R was more evident after 8 and 24 h of hypoxia in MDA-MB-231 and MCF-7 cells, whereas in HeLa cells, P2X7R expression was increased after 4 h of hypoxia. We then explored the role of HIF-1α in regulating RAGE and P2X7R expression by producing stable cell lines expressing HIF-1α shRNA. Figure 1B shows that HIF-1α-silenced cells have a small increase in HIF-1α when exposed to hypoxia for 2 and 4 h, whereas HIF-1α levels clearly increased in MDA-MB-231, HeLa and MCF-7 cells transduced with empty lentiviral particles (shEV) at the same time. We next examined the expression of RAGE and P2X7R in the HIF-1α-silenced cells under hypoxia. Furthermore, we showed (Figure 1C) that, compared with shEV-transduced cells, silencing of HIF-1α prevented RAGE and P2X7R from accumulating in the three cell lines in response to hypoxia (Figure 1C). However, we still observed a detectable increase of P2X7R after 24 h of hypoxia. The possible effects of HIF-1α silencing on other transcription factors were studied by measuring the expression of NF-κB. Figure 1D shows that, in the MDA-MB-231, HeLa and MCF-7 shEV cells, expression levels of NF-κB increased after 12 h of hypoxia and that silencing of HIF-1α reduced intracellular expression levels of NF-κB.

NF-κB regulates P2X7R expression without affecting RAGE and HIF-1α under hypoxia

NF-κB is a transcription factor playing an important role in immune responses, inflammatory diseases and cell death (35). The precise role of NF-κB in regulating the expression of P2X7R and RAGE is still not clear. Similarly, the role of NF-κB during cellular response to hypoxia is still a matter of debate with reports indicating a control of HIF-1α by NF-κB and others, instead, suggesting a regulation of NF-κB expression by HIF-1α (36). In order to clarify these two aspects, NF-κB transcription function was inhibited in MDA-MB-231, HeLa and MCF-7 cells through IKBKB silencing. IKBKB phosphorylates IkB inhibitors thereby allowing their degradation by the 26S proteasomes (37) aldose reductase. IkB degradation releases NF-κB that can translocate and accumulate into the nucleus (37). Therefore, IKBKB

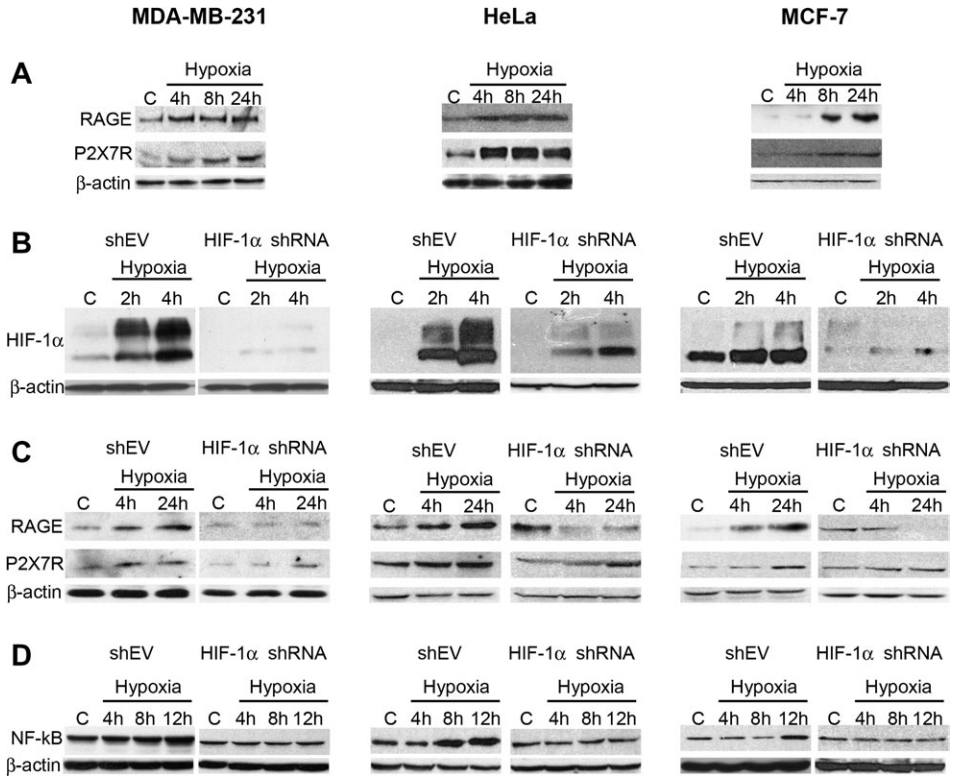

Fig. 1. HIF-1α regulation of RAGE, P2X7R and NF-κB expression levels. (**A**) MDA-MB-231, HeLa and MCF-7 cells were incubated under normoxic or hypoxic conditions. After the times indicated, cells were processed to obtain a whole cell extracts as described under 'Materials and Methods'. The contents of RAGE and P2X7R were determined by western blotting. β-Actin was used as a loading control. Blots are representative of at least three separate experiments. C, control normoxic cells. (**B**) MDA-MB-231, HeLa and MCF-7 cells either silenced for HIF-1α or transduced with lentiviral empty control particles (shEV) were incubated under normoxic or hypoxic conditions. After the times indicated, cells were processed to obtain a whole cell extracts as described under Materials and Methods. The content of HIF-1α was determined by western blotting. β-Actin was used as a loading control. Blots are representative of at least three separate experiments. C, control normoxic cells. (**C**) MDA-MB-231, HeLa and MCF-7 cells either silenced for HIF-1α or transduced with lentiviral empty control particles (shEV) were incubated under normoxic or hypoxic conditions. After the times indicated, cells were processed to obtain a whole cell extracts as described under Materials and Methods. The contents of RAGE and P2X7R were determined by western blotting. β-Actin was used as a loading control. Blots are representative of at least three separate experiments. C, control normoxic cells. (**D**) MDA-MB-231, HeLa and MCF-7 cells either silenced for HIF-1α or transduced with lentiviral empty control particles (shEV) were incubated under normoxic or hypoxic conditions. After the times indicated, cells were processed to obtain a whole cell extracts as described under Materials and Methods. The content of NF-κB was determined by western blotting. β-Actin was used as a loading control. Blots are representative of at least three separate experiments. C, control normoxic cells.

silencing keeps NF-κB in an inhibited status. Figure 2A shows the decreased expression of IKBKB in stable silenced clones obtained from the three cell lines used. We observed (Figure 2B) that, in MDA-MB-231 cells, IKBKB silencing prevented nuclear translocation of NF-κB without affecting HIF-1α stabilization and nuclear accumulation. Then, inhibition of nuclear accumulation of NF-κB prevented P2X7R upregulation after 4 and 24 h of hypoxia (Figure 2C and supplementary Figure S1, available at *Carcinogenesis* Online). Furthermore, Figure 2C and supplementary Figure S1 (available at *Carcinogenesis* Online) show that, in silenced cells, RAGE expression was still increased by 4 h of hypoxia. However, after 24 h of hypoxia, such an increase was lower than that observed in shEV-transduced cells.

RAGE and P2X7R silencing inhibits nuclear translocation of NF-κB without affecting accumulation of HIF-1α

To explore the role of the increase in RAGE and P2X7R expression observed in hypoxic cells, cell lines stably silenced for RAGE and P2X7R were produced. Figure 3A and supplementary Figure S2 (available at *Carcinogenesis* Online) show the reduction in RAGE and P2X7R expression in MDA-MB-231, HeLa and MCF-7 cells transduced with shRNA for these two receptors. We detected (Figure 3B) that exposure of shEV transduced MDA-MB-231 cells to HMGB1 and BzATP, ligands for RAGE and P2X7R, respectively, under hypoxia caused a nuclear accumulation of NF-κB. In contrast, when RAGE and P2X7R-silenced cells were treated with HMGB1 and BzATP under hypoxia, there was a reduction of nuclear NF-κB. Furthermore, we noted (Figure 3B) that BzATP still induced nuclear translocation of NF-κB in RAGE-silenced cells and, conversely, HMGB1 increased NF-κB accumulation in the nucleus of P2X7R-silenced cells. Similar results were obtained in nuclear fraction from HeLa and MCF-7 cells as shown in supplementary Figure S2, available at *Carcinogenesis* Online. In addition, Figure 3C shows that silencing RAGE or P2X7R in MDA-MB-231 cells did not alter stabilization and accumulation of HIF-1α under hypoxia similarly to what seen in shEV-transduced cells. Furthermore, addition of HMGB1 or BzATP did not change HIF-1α expression and nuclear accumulation under hypoxia (Figure 3C).

RAGE and P2X7R activation controls NF-κB nuclear accumulation and cell invasion through Akt and Erk1/2

Nuclear translocation of NF-κB is influenced by many receptor-activated intracellular signaling pathways (38). Two of the most important signaling pathways involved in cell growth and survival are the Akt and the Erk1/2 pathway. Furthermore, an increasing number of evidences indicate that both RAGE and P2X7R can activate one or both of these pathways (39–43). Since activation of Akt and Erk1/2 pathway requires phosphorylation of these proteins, we measured the levels of phospho Akt on Ser 473 and Thr 308 and of phospho Erk1/2. Figure 4A shows that hypoxia incubation of shEV-transduced MDA-MB-231 cells significantly increased phosphorylation of Akt on Ser 473 (see densitometric analysis in the figure). Addition of either HMGB1 or BzATP further increased the levels of phosphorylated Akt (Figure 4A). A similar result was obtained when measuring levels of phosphorylated Akt on Threonine 308 when, however, densitometric analysis showed that the observed increase was significant only in hypoxic cells treated with HMGB1 (Figure 4A). However, when RAGE-silenced cells were incubated in hypoxia in the presence or absence of HMGB1 or BzATP, we did not observe an increase in Akt phosphorylation on both Ser 473 and Thr 308 (Figure 4A). In P2X7R-silenced cells incubated under hypoxia in the presence or absence of BzATP, we did not observe an increase in Akt phosphorylation on Ser 473, whereas there was an increase on Thr 308 (Figure 4A). However, in these cells, there was a significant increase in phosphorylated Akt on Ser 473 in hypoxic cells treated with HMGB1 as indicated by the densitometric analysis (Figure 4A).

Here, we also examined (Figure 4B) that phosphorylation of Erk1/2 was significantly increased by hypoxia in shEV-transduced cells only in the presence of BzATP or HMGB1. RAGE silencing in MDA-MB-231 cells completely abolished hypoxia-driven phosphorylation of Erk1/2 in the presence or absence of both HMGB1 and BzATP (Figure 4B). In contrast, P2X7R silencing did not influence phosphorylation of Erk1/2 that accumulated similarly to what seen in shEV-transduced cells(Figure 4B).

The role of Akt and Erk1/2 activation was assessed by measuring both nuclear accumulation of NF-κB and cell invasion and migration.

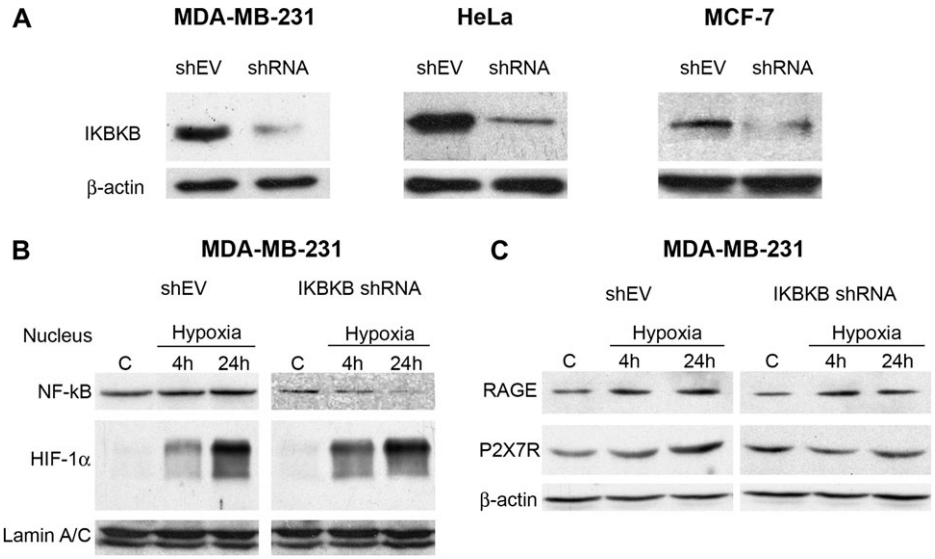

Fig. 2. NF-κB regulation of RAGE, P2X7R and HIF-1α expression levels. (**A**) MDA-MB-231, HeLa and MCF-7 cells either silenced for IKBKB or transduced with lentiviral empty control particles (shEV) were processed to obtain a whole cell extracts as described under Materials and Methods. The content of IKBKB was determined by western blotting. β-Actin was used as a loading control. Blots are representative of at least three separate experiments. (**B**) MDA-MB-231 cells either silenced for IKBKB or transduced with lentiviral empty control particles (shEV) were incubated under normoxic or hypoxic conditions. After the times indicated, cells were processed to obtain nuclear extracts as described under Materials and Methods. The nuclear contents of NF-κB and HIF-1α were determined by western blotting. Lamin was used as a loading control. Blots are representative of at least three separate experiments. C, control normoxic cells. (**C**) MDA-MB-231 cells either silenced for IKBKB or transduced with lentiviral empty control particles (shEV) were incubated under normoxic or hypoxic conditions. After the times indicated, cells were processed to obtain a whole cell extracts as described under Materials and Methods. The contents of RAGE and P2X7R were determined by western blotting. β-Actin was used as a loading control. Blots are representative of at least three separate experiments. C, control normoxic cells.

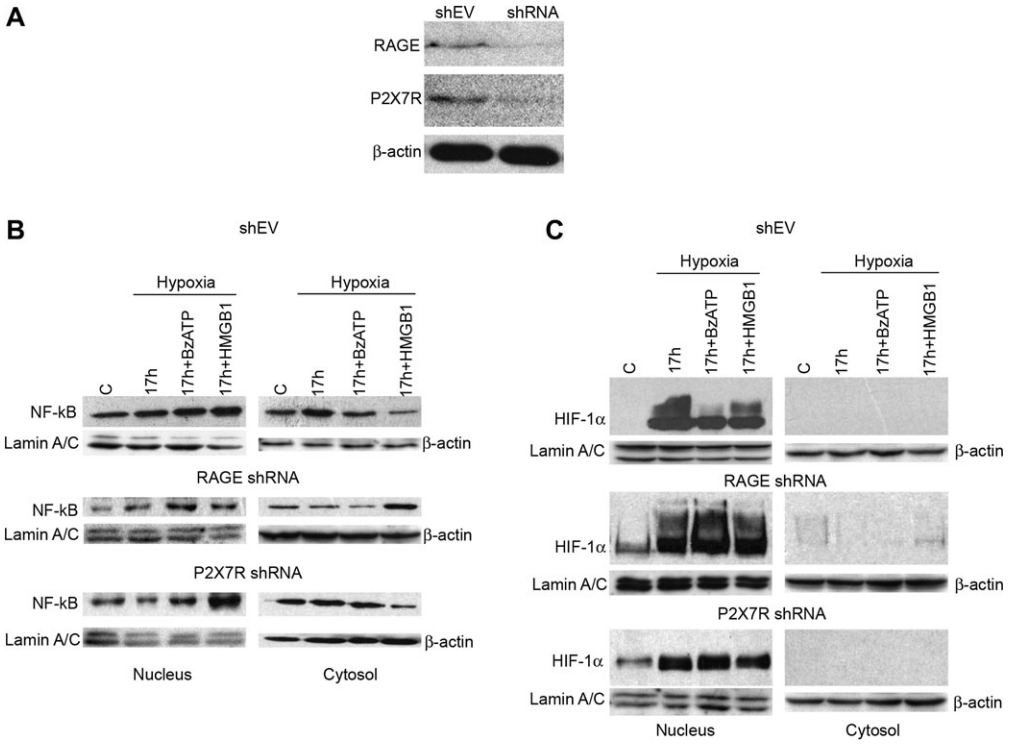

Fig. 3. RAGE and P2X7R activation regulates nuclear translocation of NF-κB under hypoxia without influencing HIF-1α. (**A**) MDA-MB-231 cells either silenced for RAGE or P2X7R or transduced with lentiviral empty control particles (shEV) were processed to obtain a whole cell extracts as described under Materials and Methods. The contents of RAGE or P2X7R were determined by western blotting. β-Actin was used as a loading control. Blots are representative of at least three separate experiments. (**B**) MDA-MB-231 cells either silenced for RAGE or P2X7R or transduced with lentiviral empty control particles (shEV) were incubated under normoxic or hypoxic conditions. While under hypoxia, cells were either left untreated or treated with BzATP or HMGB1. After 17 h, cells were processed to obtain nuclear and cytosolic fractions as described under Materials and Methods. The content of NF-κB was determined by western blotting. β-Actin and Lamin A/C were used as a loading control for the cytosolic and nuclear fraction, respectively. Blots are representative of at least three separate experiments. C, control normoxic cells. (**C**) MDA-MB-231 cells either silenced for RAGE or P2X7R or transduced with lentiviral empty control particles (shEV) were incubated under normoxic or hypoxic conditions. While under hypoxia, cells were either left untreated or treated with BzATP or HMGB1. After 4 h, cells were processed to obtain nuclear and cytosolic fractions as described under Materials and Methods. The content of HIF-1α was determined by western blotting. β-Actin and Lamin A/C were used as a loading control for the cytosolic and nuclear fraction, respectively. Blots are representative of at least three separate experiments. C, control normoxic cells.

Western blot of nuclear NF-κB and the densitometric analysis relative to the nuclear marker Lamin A/C were performed. Figure 4C shows that inhibition of Akt by the cell permeable-specific inhibitor SH5 and Erk1/2 by the cell permeable inhibitor INH1 significantly prevented nuclear accumulation of NF-κB in the presence of hypoxia or hypoxia and BzATP or HMGB1. Moreover, Supplementary Figure S3 (available at *Carcinogenesis* Online) shows that inhibition of Akt or Erk1/2 in MDA-MB-3231 and HeLa cells prevented invasion of extracellular matrigel and migration through the membrane pores.

RAGE and P2X7R influence cell invasion and activation of MMP-2 and -9

Biological effects of RAGE and P2X7R silencing were evaluated by measuring invasion ability of shEV transduced and silenced clones of hypoxic MDA-MB-231, HeLa and MCF-7 cells in the presence or absence of HMGB1 and BzATP. Figure 5A shows that hypoxia increased the number of invading shEV-transduced cells and that both HMGB1 and BzATP caused a further increase of invading cells. In contrast, RAGE-silenced cells did not show any increased invasion ability under hypoxia. Addition of HMGB1 did not increase invasion. However, treatment with BzATP restored invasion of these cellular clone (Figure 5A). Similarly, hypoxia did not increase invasion of P2X7R-silenced cells even in the presence of BzATP. However, addition of HMGB1 restored invasion of these silenced clone (Figure 5A). It is worth noting that silencing RAGE or P2X7R reduced invasion of normoxic-untreated cells (Figure 5A).

Figure 5B and supplementary Figure S4 (available at *Carcinogenesis* Online) show colorimetric analysis measured at 560 nm of stained MDA-MB-231, HeLa and MCF-7 cells from three different experiments similar to the one shown in Figure 5A. In these three cell lines, hypoxia-increased invasion was further enhanced by BzATP or HMGB1 addition. Importantly, RAGE silencing prevented cellular invasion under hypoxia or hypoxia and HMGB1 but not under hypoxia plus BzATP. P2X7R silencing significantly reduced cellular invasion under hypoxia but not under hypoxia plus HMGB1. Finally, P2X7R silencing inhibited the increase in invasion in the presence of BzATP only in hypoxic MCF-7 cells (Supplementary Figure S4 is available at *Carcinogenesis* Online).

Digestion of the extracellular matrix is a crucial step in tumor cell invasion and metastasis. This process is carried out by matrix metalloproteinases, mainly MMP-2 and MMP-9. The effects of hypoxia on MMP-2 and -9 activity and the quantitative analysis of such effects in shEV transduced, RAGE and P2X7R-silenced MDA-MB-231, HeLa and MCF-7 cells are shown in Figure 6. In shEV-transduced cells, hypoxia significantly increased activity of MMP-2 and MMP-9. Silencing of RAGE caused a reduction of MMP-9 activity and a small reduction of MMP-2 activity when compared with shEV-transduced cells (Figure 6). Similarly, silencing P2X7R significantly decreased activity of MMP-9, whereas MMP-2 activity showed a minor increase (Figure 6).

Discussion

The present study demonstrates that the alarmin receptors RAGE and P2X7R are required to maintain invasion of tumor cells in the presence of hypoxic stress. Additionally, we show that, once activated by HMGB1 or BzATP, RAGE and P2X7R initiate a signaling pathway involving phosphorylation of Akt and Erk1/2 and nuclear

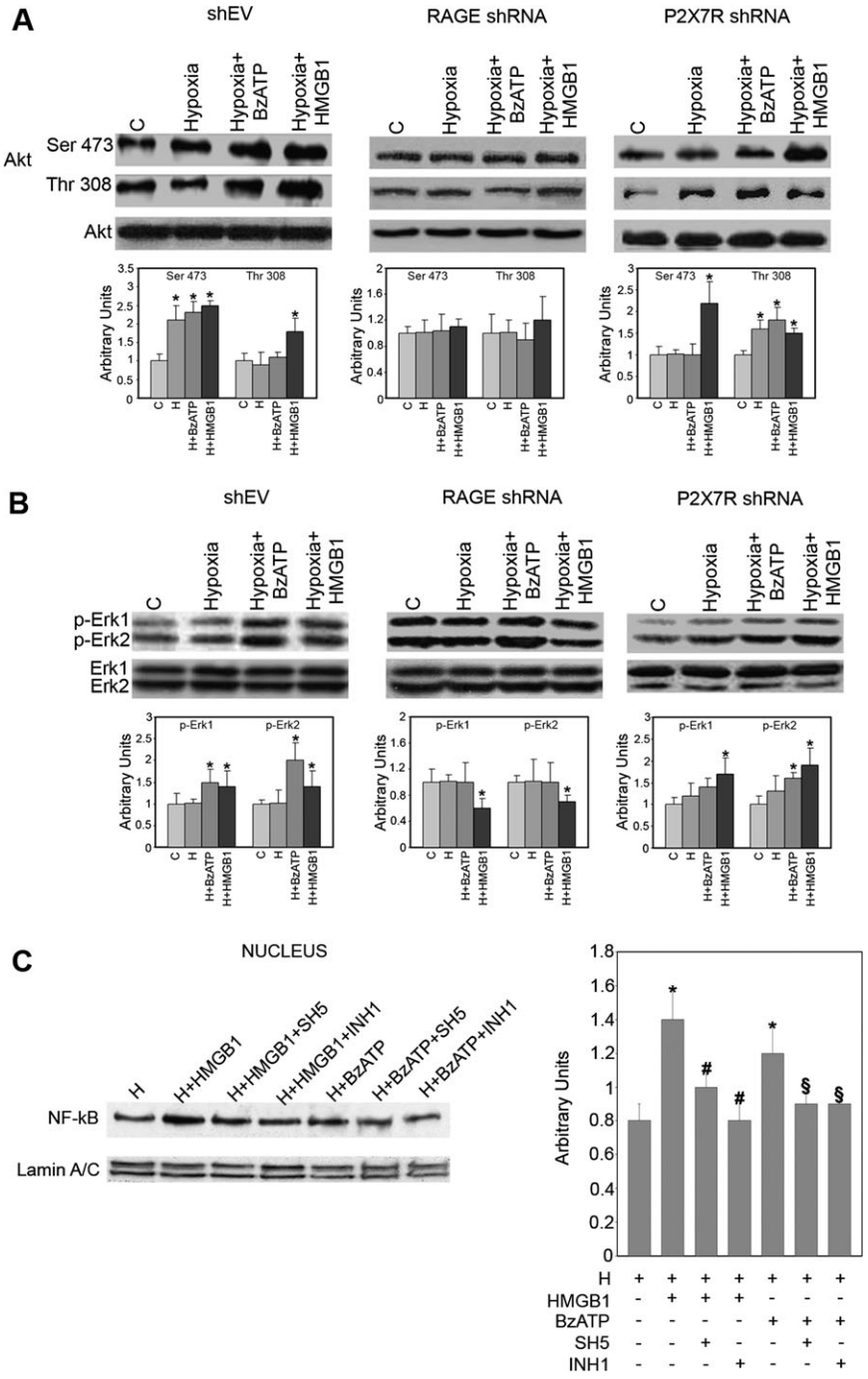

Fig. 4. Akt and Erk1/2 kinases are involved in RAGE and P2X7R signaling and control NF-κB nuclear accumulation. (**A**) MDA-MB-231 cells either silenced for RAGE or P2X7R or transduced with lentiviral empty control particles (shEV) were incubated under normoxic or hypoxic conditions. One hour prior the end of hypoxia treatment, BzATP or HMGB1 were added. Alternatively, hypoxic cells were left untreated. Afterward, cells were processed to obtain a whole cell lysate. Phosphorylation levels of Akt on Ser 473 and Thr 308 as well as total Akt levels were determined by western blotting. Densitometric analysis was calculated from three separate blots as described under Materials and Methods. Values are represented as mean ± SD. $^{*}P < 0.05$. (**B**) MDA-MB-231 cells either silenced for RAGE or P2X7R or transduced with lentiviral empty control particles (shEV) were incubated under normoxic or hypoxic conditions. One hour prior the end of hypoxia treatment, BzATP or HMGB1 were added. Alternatively, hypoxic cells were left untreated. Afterward, cells were processed to obtain a whole cell lysate. Phosphorylation levels of Erk1/2 as well as total Erk1/2 levels were determined by western blotting. Densitometric analysis was calculated from three separate blots as described under Materials and Methods. Values are represented as mean ± SD. $^{*}P < 0.05$. (**C**) MDA-MB-231 cells were pretreated with Akt inhibitor SH5 or Erk inhibitor INH1 for 1 h. Afterward, cells were incubated under hypoxia in the presence of either BzATP or HMGB1 for 17 h. Alternatively, cells were left untreated for 17 h under hypoxia. At the end of the hypoxic treatment, nuclear fractions were obtained and lysed as described under Materials and Methods. NF-κB levels were measured by western blotting. Lamin A/C was used as a loading control for the nuclear fraction. Densitometric analysis of NF-κB relative to Lamin A/C was calculated from three separate blots as described under Materials and Methods. Values are represented as mean ± SD. *, significantly different from hypoxia. #, significantly different from HMGB1. §, significantly different from BzATP. $P < 0.05$. H, hypoxia.

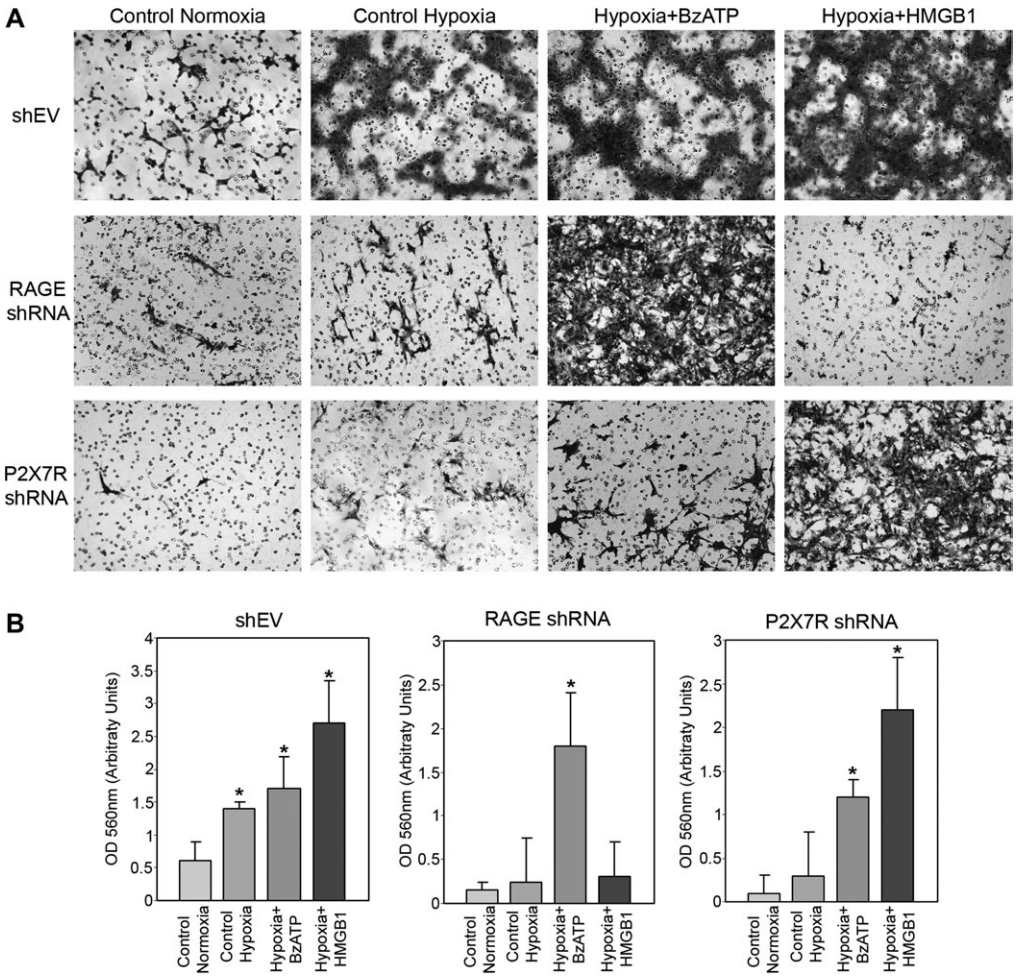

Fig. 5. RAGE and P2X7R control invasion of hypoxic MDA-MB-231 cells. (**A**) MDA-MB-231 cells either silenced for RAGE or P2X7R or transduced with lentiviral empty control particles (shEV) were incubated under normoxic or hypoxic conditions. While under hypoxia, cells were either left untreated or treated with BzATP or HMGB1 for 48 h. Invasion of cells through the matrigel was assessed by staining invading cells as described under Materials and Methods. Pictures of the cells at the bottom of the membrane were taken at ×20 with a digital camera mounted on an EclipseNet 2000 microscope. (**B**) MDA-MB-231 cells either silenced for RAGE or P2X7R or transduced with lentiviral empty control particles (shEV) were treated as described in A. Stained cells were dissolved as described under Materials and Methods and color intensity measured by reading the OD at 560 nm. Values are represented as mean ± SD. $^{*}P < 0.05$.

translocation of NF-κB. Once in the nucleus, NF-κB would maintain the increased expression of RAGE and P2X7R as well as of MMP-2 and -9, thereby contributing to invasion and survival of tumor cells.

RAGE is a membrane receptor expressed by a variety of cell types (6–11). Blockade of RAGE signaling has been shown to reduce tumor growth and tumor cell invasion (21). In neurons, RAGE expression is increased following hypoxia/ischemia and such an increase is transcriptionally controlled by HIF-1α (4). At the same time, RAGE is overexpressed in many tumors and tumor-associated cells and its presence has a pivotal role in linking chronic inflammation with tumor development (15–17).

P2X7R is considered by many as a typical cytotoxic receptor. P2X7R activation induces apoptosis in several leukemia cell lines (26,30), macrophages (44), thymocytes (45) and epithelial cancer cells (27) via different mechanisms involving formation of a cytolytic pore, increased Ca^{+} influx or *de novo* synthesis of ceramide and mitochondria involvement (45,46). In contrast, accumulating experimental evidence suggests a proliferative and prosurvival role for P2X7R (31). In fact, P2X7R increases osteoclast formation and activity through activation of NF-κB (47), survival of cerebellar granules neurons via GSK3 phosphorylation (33) as well as promoting serum-independent growth (31). Moreover, P2X7R stimulates migration of C6 glioma cells (48) and is upregulated in many tumors including chronic B lymphocytic leukemia, prostate carcinoma, neuroblastoma and thyroid papillary cancer (31,49).

Both RAGE and P2X7R are DAMPs receptors highly expressed in immune cells and capable of coordinating the activation of different transcription factors within the cell. RAGE and P2X7R signaling pathways proceed through diverging and common roads that, however, converge on the transcription factor NF-κB. In fact, both receptors, once bound to their ligands, activate intracellular kinases that phosphorylates a plethora of substrates. In particular, RAGE signals through Akt, Erk1/2, p38 and other kinases to activate NF-κB (17). Similarly, both the PI3-kinase/Akt and the ERK1/2 pathway are activated by P2X7R (33). In this case, however, Akt phosphorylation of GSK3 would regulate the cytotoxic or survival effects of this receptor (33). In fact, phosphorylated GSK3 would not activate the proapoptotic protein Bax, thereby increasing cell survival (33). Therefore, the possible cytotoxic effects of P2X7R that are not present with RAGE represent the most important difference between these two receptors. However, here we demonstrate that, under the physiological conditions of hypoxia, P2X7R expression increases and, through Akt activation, promotes cellular invasion. It is also important to notice that such increased RAGE and P2X7R expression has been observed by us in many different human tumor biopsies such as breast, prostate and glioblastoma (34).

The present study shows that both RAGE and P2X7R are overexpressed in MDA-MB-231, HeLa and MCF-7 cells after hypoxic stress (Figure 1). Furthermore, increased RAGE and P2X7R expression is necessary for cellular invasion in the presence of a ligand such as

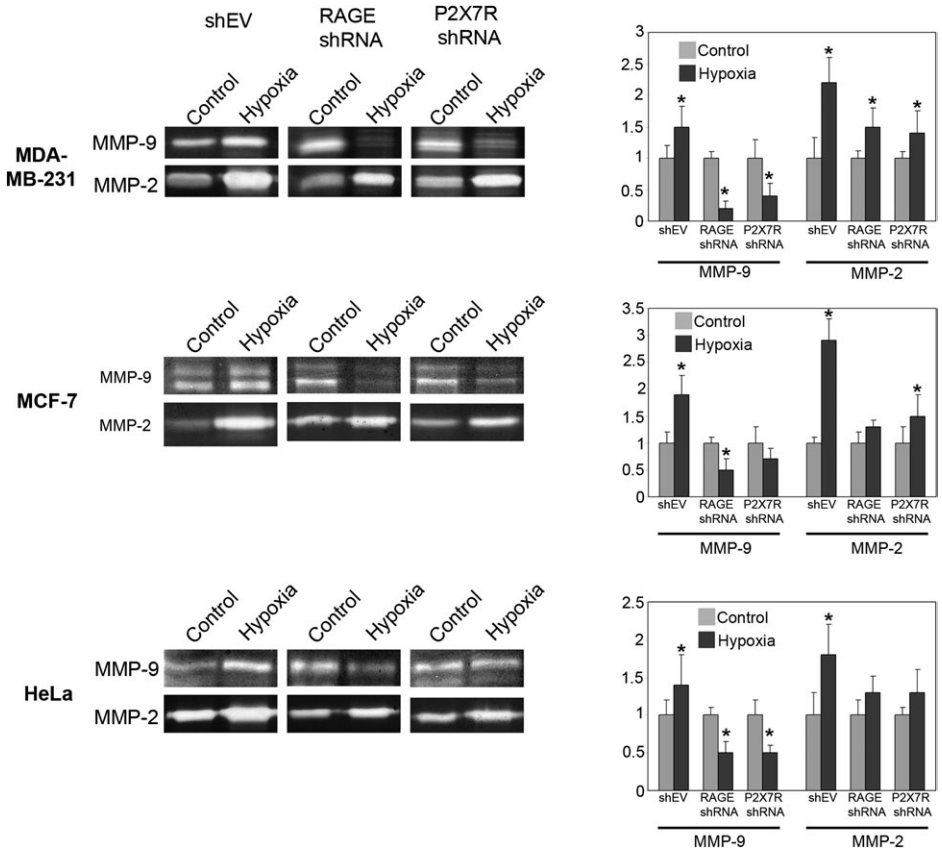

Fig. 6. MMP-2 and MMP-9 activity in RAGE- and P2X7R-silenced cells. MDA-MB-231, HeLa and MCF-7 cells either silenced for RAGE or P2X7R or transduced with lentiviral empty control particles (shEV) were incubated under normoxic or hypoxic conditions for 48 h. MMP-2 and MMP-9 activity was measured by zymography as described under Materials and Methods. Densitometric analysis was calculated from three separate blots as described under Materials and Methods. Values are represented as mean ± SD. $^{*}P < 0.05$.

HMGB1 or BzATP (Figure 5 and supplementary Figure S4, available at *Carcinogenesis* Online) by initiating an intracellular pathway involving phoshorylation of Akt and Erk1/2 and leading to NF-κB nuclear accumulation which, in turn, sustains expression of MMPs. Importantly, these events were abolished in the three cell lines used when Akt or Erk1/2 were inhibited or when RAGE or P2X7R expression was stably silenced. However, the most prominent effects on cell invasion were observed when manipulating RAGE pathway. Therefore, our results indicate that hypoxia-increased RAGE and P2X7R expression in transformed cells may be important for tumor malignancy because of the ability of transformed cells to respond to extracellular signals, such as HMGB1, S100 proteins and ATP released by necrotic cells.

By using three different cell lines (MDA-MB-231, HeLa and MCF-7), we aimed to demonstrate that, at least in the presence of hypoxia stimulus, the increase in P2X7R expression plays a role in inducing cell invasion in the presence of extracellular ligands such us ATP without causing any massive cell death. We also show that the pathway activated by P2X7R proceeds through phosphorylation of Akt and nuclear accumulation of NF-κB. In fact, silencing P2X7R resulted in an inhibition of Akt phosphorylation, absence of NF-κB nuclear translocation and abolished cell invasion.

Our study shed light also on the role of NF-κB and HIF-1α in the cellular response to hypoxia. In fact, we have shown that in MDA-MB-231, HeLa and MCF-7 cell lines silencing of HIF-1α reduced hypoxia-driven accumulation of NF-κB. In contrast, IKBKB silencing did not affect hypoxia-driven HIF-1α accumulation in MDA-MB-231 cells. This suggests that, when cells are under hypoxia, HIF-1α controls transcription of NF-κB. These results, in light of what shown previously by us in breast tumor samples (19), demonstrate that activation of HIF-1α in hypoxic regions of human tumors controls the activation and nuclear translocation of NF-κB.

Furthermore, our results show that both HIF-1α and NF-κB collaborate in sustaining the overexpression of membrane receptors such as RAGE and P2X7R in hypoxic cells.

In the case of the inner region of a fast growing primary tumor, the situation is not as linear as in the case of a cell line and many cells in different tumor regions will die by necrosis because of the lack in oxygen. However, the tumor is composed of regions with different oxygen tension and vascularization in which HIF activation is best represented by a gradient and not by an on/off situation. In this case, therefore, there is the formation of so-called hypoxic niches in which some cells are necrotic and some others are still vital. We believe that these tumor cells are the ones that, by expressing RAGE and P2X7R, along with other membrane receptors, have the potential to migrate to the external regions of the tumor-initiating tumor progression. Moreover, we hypothesize that, in the tumor, these cells are mostly represented by tumor stem cells. In fact, recently, we have published a paper on glioblastoma multiforme in which we demonstrate that the expression of RAGE and P2X7R is greatly stimulated by hypoxia in tumor stem cells and reduced when these cells are differentiated *in vitro* (34).

A schematic illustration of the response of transformed cells to hypoxic stimulus is drawn in supplementary Figure S5 (available at *Carcinogenesis* Online). Hypoxia increases expression levels of the membrane receptors RAGE and P2X7R through HIF-1α first and then through HIF-1α-dependent increase of NF-κB. At the same time, HIF-1α increases activity of MMPs and particularly MMP-9. In the presence of exogenously added ligands such as HMGB1 and BzATP or of necrosis, normally present in the inner region of the growing tumor, these cells activates signaling pathways that, from RAGE and P2X7R ultimately, lead to NF-κB nuclear accumulation. Once in the nucleus, NF-κB helps in maintaining expression of RAGE and P2X7R

as well as MMP-2 and -9 and other genes related to invasion and survival thereby increasing the possibility of tumor progression.

Supplementary material

Supplementary Figures S1–S5 can be found at http://carcin.oxfordjournals.org/

Funding

This work was partially supported by Italian Ministry of Health grant RFPS-2006-7-342220.

Conflict of Interest Statement: None declared.

References

1. Semenza,G.L. (2007) Hypoxia-inducible factor 1 (HIF-1) pathway. *Sci. STKE*, **407**, cm8.
2. Irwin,D.C. *et al*. (2009) A potential role for reactive oxygen species and the HIF-1alpha-VEGF pathway in hypoxia-induced pulmonary vascular leak. *Free Radic. Biol. Med.*, **47**, 55–61.
3. Song,I.S. *et al*. (2009) Regulation of glucose metabolism-related genes and VEGF by HIF-1alpha and HIF-1beta, but not HIF-2alpha, in gastric cancer. *Exp. Mol. Med.*, **41**, 51–58.
4. Pichiule,P. *et al*. (2007) Hypoxia-inducible factor-1 mediates neuronal expression of the receptor for advanced glycation end products following hypoxia/ischemia. *J. Biol. Chem.*, **282**, 36330–36340.
5. Kono,H. *et al*. (2008) How dying cells alert the immune system to danger. *Nat. Rev. Immunol.*, **8**, 279–289.
6. Ramasamy,R. *et al*. (2009) RAGE: therapeutic target and biomarker of the inflammatory response–the evidence mounts. *J. Leukoc. Biol.*, **86**, 505–512.
7. Ohashi,K. *et al*. (2010) Advanced glycation end products enhance monocyte activation during human mixed lymphocyte reaction. *Clin. Immunol.*, **134**, 345–353.
8. Hasegawa,T. *et al*. (2003) The regulation of EN-RAGE (S100A12) gene expression in human THP-1 macrophages. *Atherosclerosis*, **171**, 211–218.
9. Zhou,Z. *et al*. (2006) Regulation of osteoclast function and bone mass by RAGE. *J. Exp. Med.*, **203**, 1067–1080.
10. Kuniyasu,H. *et al*. (2002) Expression of receptors for advanced glycation end-products (RAGE) is closely associated with the invasive and metastatic activity of gastric cancer. *J. Pathol.*, **196**, 163–170.
11. Kuniyasu,H. *et al*. (2003) Co-expression of receptor for advanced glycation end products and the ligand amphoterin associates closely with metastasis of colorectal cancer. *Oncol. Rep.*, **10**, 445–448.
12. Vicente Miranda,H. *et al*. (2010) The sour side of neurodegenerative disorders: the effects of protein glycation. *J. Pathol.*, **221**, 13–25.
13. Kim,W. *et al*. (2005) Receptor for advanced glycation end products and its ligands: a journey from the complications of diabetes to its pathogenesis. *Ann. N. Y. Acad. Sci.*, **1043**, 553–561.
14. Logsdon,C.D. *et al*. (2007) RAGE and RAGE ligands in cancer. *Curr. Mol. Med.*, **7**, 777–789.
15. Gebhardt,C. *et al*. (2008) RAGE signaling sustains inflammation and promotes tumor development. *J. Exp. Med.*, **205**, 275–285.
16. Sparvero,L.J. *et al*. (2009) RAGE (Receptor for Advanced Glycation Endproducts), RAGE ligands, and their role in cancer and inflammation. *J. Transl. Med.*, **7**, 17.
17. Riehl,A. *et al*. (2009) The receptor RAGE: bridging inflammation and cancer. *Cell Commun. Signal.*, **7**, 12.
18. Ravenna,L. *et al*. (2009) Up-regulation of the inflammatory-reparative phenotype in human prostate carcinoma. *Prostate*, **69**, 1245–1255.
19. Tafani,M. *et al*. (2010) Up-regulation of pro-inflammatory genes as adaptation to hypoxia in MCF-7 cells and in human mammary invasive carcinoma microenvironment. *Cancer Sci.*, **4**, 1014–1023.
20. Abe,R. *et al*. (2008) AGE-RAGE system and carcinogenesis. *Curr. Pharm. Des.*, **14**, 940–945.
21. Taguchi,A. *et al*. (2000) Blockade of RAGE-amphoterin signalling suppresses tumour growth and metastases. *Nature*, **405**, 354–360.
22. North,R.A. (2002) Molecular physiology of P2X receptors. *Physiol. Rev.*, **82**, 1013–1067.
23. Surprenant,A. *et al*. (2009) Signaling at purinergic P2X receptors. *Annu. Rev. Physiol.*, **71**, 333–359.
24. Amstrup,J. *et al*. (2003) P2X7 receptor activates extracellular signal-regulated kinases ERK1 and ERK2 independently of Ca2+ influx. *Biochem. J.*, **374**, 51–61.
25. Jacobson,K.A. *et al*. (2006) Agonists and antagonists for P2 receptors. *Novartis Found. Symp.*, **276**, 58–68.
26. Zhang,X. *et al*. (2009) The role of P2X7 receptor in ATP-mediated human leukemia cell death: calcium influx-independent. *Acta Biochim. Biophys. Sin. (Shanghai)*, **41**, 362–369.
27. Gorodeski,G.I. (2009) P2X7-mediated chemoprevention of epithelial cancers. *Expert Opin. Ther. Targets*, **13**, 1313–1332.
28. Wen,L.T. *et al*. (2003) Extracellular ATP and adenosine induce cell apoptosis of human hepatoma Li-7A cells via the A3 adenosine receptor. *Br. J. Pharmacol.*, **140**, 1009–1018.
29. Fu,W. *et al*. (2009) Activation of P2X(7)-mediated apoptosis Inhibits DMBA/TPA-induced formation of skin papillomas and cancer in mice. *BMC Cancer*, **9**, 114.
30. Bernardo,A.A. *et al*. (2006) Effect of extracellular ATP on the human leukaemic cell line K562 and its multidrug counterpart. *Mol. Cell. Biochem.*, **289**, 111–124.
31. Di Virgilio,F. *et al*. (2009) P2X(7): a growth-promoting receptor-implications for cancer. *Purinergic Signal.*, **5**, 251–256.
32. Adinolfi,E. *et al*. (2009) Expression of the P2X7 receptor increases the Ca2+ content of the endoplasmic reticulum, activates NFATc1, and protects from apoptosis. *J. Biol. Chem.*, **284**, 10120–10128.
33. Ortega,F. *et al*. (2010) P2X7, NMDA and BDNF receptors converge on GSK3 phosphorylation and cooperate to promote survival in cerebellar granule neurons. *Cell. Mol. Life Sci.*, **67**, 1723–1733.
34. Tafani,M. *et al*. (2011) Pro-inflammatory gene expression in solid glioblastoma microenvironment and in hypoxic stem cells from human glioblastoma. *J Neuroinflammation*, **8**, 32.
35. Karin,M. *et al*. (2002) NF-kappaB in cancer: from innocent bystander to major culprit. *Nat. Rev. Cancer*, **2**, 301–310.
36. Rius,J. *et al*. (2008) NF-kappaB links innate immunity to the hypoxic response through transcriptional regulation of HIF-1alpha. *Nature*, **453**, 807–811.
37. Schmid,J.A. *et al*. (2008) IkappaB kinase beta (IKKbeta/IKK2/IKBKB)–a key molecule in signaling to the transcription factor NF-kappaB. *Cytokine Growth Factor Rev.*, **19**, 157–165.
38. Lin,Y. *et al*. (2010) The NF-kappaB activation pathways, emerging molecular targets for cancer prevention and therapy. *Expert Opin. Ther. Targets*, **14**, 45–55.
39. Riuzzi,F. *et al*. (2007) RAGE expression in rhabdomyosarcoma cells results in myogenic differentiation and reduced proliferation, migration, invasiveness, and tumor growth. *Am. J. Pathol.*, **171**, 947–961.
40. Ranzato,E. *et al*. (2010) Hmgb1 promotes wound healing of 3T3 mouse fibroblasts via rage-dependent ERK1/2 activation. *Cell Biochem. Biophys.*, **57**, 9–17.
41. Touré,F. *et al*. (2008) Receptor for advanced glycation end-products (RAGE) modulates neutrophil adhesion and migration on glycoxidated extracellular matrix. *Biochem. J.*, **416**, 255–261.
42. Jacques-Silva,M.C. *et al*. (2004) P2X7 receptors stimulate AKT phosphorylation in astrocytes. *Br. J. Pharmacol.*, **141**, 1106–1117.
43. Mistafa,O. *et al*. (2008) Statins and ATP regulate nuclear pAkt via the P2X7 purinergic receptor in epithelial cells. *Biochem. Biophys. Res. Commun.*, **365**, 131–136.
44. Le Stunff,H. *et al*. (2007) P2X7 receptor-mediated phosphatidic acid production delays ATP-induced pore opening and cytolysis of RAW 264.7 macrophages. *Cell Signal.*, **19**, 1909–1918.
45. Lépine,S. *et al*. (2006) ATP-induced apoptosis of thymocytes is mediated by activation of P2 X 7 receptor and involves de novo ceramide synthesis and mitochondria. *Biochim. Biophys. Acta*, **1761**, 73–82.
46. Raymond,M.N. *et al*. (2006) Involvement of de novo ceramide biosynthesis in macrophage death induced by activation of ATP-sensitive P2X7 receptor. *FEBS Lett.*, **580**, 131–136.
47. Korcok,J. *et al*. (2004) Extracellular nucleotides act through P2X7 receptors to activate NF-kappaB in osteoclasts. *J. Bone Miner. Res.*, **19**, 642–651.
48. Wei,W. *et al*. (2008) Expression and function of the P2X(7) receptor in rat C6 glioma cells. *Cancer Lett.*, **260**, 79–87.
49. Solini,A. *et al*. (2008) Increased P2X7 receptor expression and function in thyroid papillary cancer: a new potential marker of the disease? *Endocrinology*, **149**, 389–396.

Received November 24, 2010; revised May 10, 2011; accepted May 28, 2011